34th Annual International Conference of the IEEE EMBS
San Diego, California USA, 28 August - 1 September, 2012

Acoustic interrogation and optical visualization of ultrasound contrast agents within microcapsules

P. Santhiranayagam, S. Thirumalai, F. Memom, Y. Shan, S. J. Lee, M. Mobed-Miremadi and M. Keralapura

Abstract— **The effectiveness of localized drug delivery as a treatment for breast cancer requires sufficiently high therapeutic dose, as well as an ability to image the drug for proper spatial targeting. To balance treatment potential and imaging capabilities, we have begun to design a novel drug reservoir using microcapsules that are large in size (> 30 µm) but functionalized with microbubbles or ultrasound contrast agents (UCAs). We term these carriers as 'Acoustically Sensitive Microcapsules' (ASMs). In previous work, we have demonstrated preparation of ASM carriers and their structural changes under therapeutic ultrasound by imaging static changes. In this paper, we describe a combined optical-acoustic setup coupled with a microfluidic device to trap these carriers for imaging and sonication. Using the setup, continuous wave ultrasound (180 kPa, 2.25 MHz, 3 s) produced an average displacement of 3.5 µm in UCAs near the ASM boundary, and exhibited displacement as high as 90 µm near the center of the microcapsule. Longer exposure time and higher acoustic pressure increased UCA displacement within an ASM. These two parameters can be carefully optimized in the future to cause these UCAs to travel to the membrane boundary to help in the drug elution process.**

I. Introduction

Research in localized drug delivery for breast cancer treatment is exploring nano-microparticulate carriers to improve the therapeutic dose delivered to the tumor with minimum toxicity [1]. Among several of these agents are a group of ultrasound carriers like targeted microbubbles (~2 µm) [2], acoustic lipospheres (~1.6 µm) [3] and nano-droplets (~100 nm). These delivery vehicles belong to new paradigm of localized treatments that integrate therapeutic interventions with diagnostic imaging. In this method, ultrasound is first used in a diagnostic image-guidance mode (low energy) to locate these carriers in the tumor. Subsequently ultrasound in therapeutic triggered mode (high energy) destroys the carrier to release its payload [4].

Microbubbles provide excellent contrast for image guidance, but have short circulation times (<1 hr) and require frequent dosing [4]. Also they cannot cross the endothelial wall because of their size [4]. Nano-ultrasound carriers [1, 4] on the other hand, have longer circulation times (24-48 hr) [1], extravasate well providing adequate dose, but have poorer imaging contrast.

To balance both treatment potential and imaging capabilities, we have begun to design a novel drug reservoir using microcapsules that are large in size (> 30 µm) but functionalized with microbubbles or ultrasound contrast agents (UCAs). We term these carriers as 'Acoustically Sensitive Microcapsules' or ASMs and these are not meant to be introduced into the circulation but rather to be intra-tumorally injected into breast tumors.

Microcapsules have been used most commonly in cell encapsulation for treatment metabolic disorders [5]. They have been shown to be biocompatible and patent in form and function for up to 20 weeks after implantation [5]. Microcapsules can be simply injected as they difficult to mechanically disrupt and their size can be tailored from a few µm-mm. They offer other advantages like high drug payloads, surface modification capabilities and are highly reproducible [5].

We have demonstrated in previous work [6], the design and preparation of ASM carriers and their structural changes under therapeutic ultrasound. The UCAs encapsulated within ASMs provided a nucleus for ultrasound stimulus responsiveness and membrane damage for release of payload. ASMs prepared without UCAs within them showed no responsiveness to similar levels of therapeutic ultrasound.

The previous work involved immobilizing ASMs within transparent gelatin media and visualizing membrane damage using light transmission or fluorescence microscopy before and after therapeutic ultrasound exposure. This static setup did not allow for visualizing the real-time behavior of the UCAs within the ASMs and how they modulated membrane changes and payload release. Repeating the experiment on the microscope with a high-speed camera still did not allow for reliable visualization of the UCAs within the ASMs. This was primarily due to the fact that the size/shape of the ASMs is large and spherical and the microscope essentially captures only a single slice through the carrier and any vertical movement of the UCAs was seen as being transient and could not be tracked.

In this paper, we describe a novel setup for real-time visualization of UCA movement within these acoustically sensitive microcapsules to understand how UCA movement can be facilitated using therapeutic ultrasound. This will be used in the future to investigate how UCAs cause payload release from ASMs. We describe a combined optical-acoustic setup coupled with a microfluidic device to trap the carrier for visualization and sonication.

*Research supported by Jr. Professorship Grant, SJSU, College of
J. Lee is a faculty in the Mechanical Engineering department, director of the microfluidics lab, SJSU. M. Mobed-Miremadi is a faculty in the Biomedical Engineering department, director of the bioengineering lab, SJSU. M. Keralapura is a faculty in the Electrical Engineering department, SJSU and director of the biomedical systems lab. She is the corresponding author on this work. Email: Mallika.keralapura@sjsu.edu.

II. METHODS

A. Preparation of Acoustically Sensitive Microcapsules

Microencapsulation is an immobilization process by which a biomaterial is enclosed in a polymeric matrix surrounded by a membrane. Alginate microcapsules are used extensively because of the controllable range of membrane permeability and the ease for solvent free microcapsule synthesis steps conducted at the physiological pH of 7.4. All chemicals used to make the microcapsules were purchased from Sigma Aldrich. ASMs were prepared using atomization techniques [6] and inkjet techniques. Atomization creates microcapsules in the range of 300-1000 μm and inkjet creates ASMs in the range of 30-100 μm. The ASMs were designed such that their size was large enough for encapsulating UCAs along with a drug-like substance. To create ASMs, drug-like substance (ex. blue dextran) along with UCAs (Targestar-P) was suspended in sodium alginate. For a given viscosity, the coaxial airflow in the atomizer shears the sodium alginate/UCA mixture into droplets. The size of the droplets was controlled by the air and suspension flow-rate along with the dimensions of the atomizer. The atomizer needle assembly is a concentric 24G stainless steel (SS) needle surrounded by a 16 G SS needle. Typically, a 2 % sodium-alginate solution (μ=500 cP (formulation viscosity), γ=45 dyn.cm (surface tension) containing a 10 % (v/v) solution of UCAs (2 ± 0.5 μm) was atomized into a 1.5 % $CaCl_2$ bath. The resulting suspension was then suspended in a 55 mM sodium citrate solution for 30 seconds in order to liquefy the alginate core. Microcapsules in the range of 30-100 μm were fabricated using our ink-jet system and the details are presented in [6]. In this paper, we use only microcapsules > 300 μm from the Atomizer.

B. Design of the Microfluidic Device

To overcome visualization difficulties, we designed a microfluidic device to trap ASMs and placed this unit within a small water tank on the microscope for ultrasound exposure. The device was designed with a height of 40μm with the main purpose of compressing the ASMs within it from a sphere to a flat disc during the microfluidic bonding process. This decrease in height allows for better visualization of ultrasound activity, since, all activity that was occurring in the large 3D spherical volume (the ASM) is now forced to occur in the plane of the microscope within the ASM. The methods section below describes the design of the microfluidics device and ultrasound exposure of ASMs within the microfluidics device.

B.1. Device Fabrication Process

Micro-flow channels were fabricated by using a series of casting and molding techniques. The mold was fabricated with a single layer SU-8 (SU-8 2035, Micro-Chem Corp.) spin coated on a silicon wafer. The designed geometric features of the microfluidic device were transferred to the mold by creating a photo-mask, drafted using AutoCAD software. The layout of the mask is shown in Figure 1a. The mask was fabricated by laser photo-plotting onto a 175 μm film with 20,000 DPI resolution.

The substrate was soft baked for 3 min at 65 °C followed by 9 min at 95 °C and then exposed to a UV light source (power = 4.45 mW/cm^2, exposure time = 36.4 seconds) using a Quintel Q4000 contact aligner (Neutronix, Inc.) under the photo-mask shown in Figure 1a. To ensure that the fabricated sidewalls of the SU-8 mold were vertical an UV filter that eliminated radiation below 350 nm wavelength was used. The wafer was removed from the hotplate and allowed to cool down to room temperature for a few minutes. The cooled wafer was then developed in a SU-8 developer solution (MicroChem Corp.) for approximately 7 min followed by drying with compressed air.

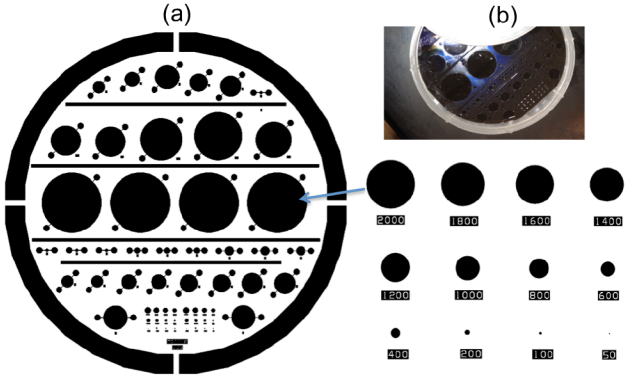

Figure 1: (a) Photomask with pallete of wells (dimensions in microns) (b) SU-8 Wafer

The completed SU-8 mold is shown in Figure 1b. A cross section profile of the fabricated SU-8 region was imaged using a Wyko NT9100 optical profiler (Veeco Instruments Inc.). The actual fabricated height was 36.4 μm. After the SU-8 mold was fabricated, it was vapor treated to facilitate easy peeling during casting technique. The liquid polydimethylsiloxane (PDMS, Sylgard 184 from Dow Corning Corp.) along with its curing agent (Sylgard 184 Silicone elastomer kit) were mixed in a ratio of 5:1 by weight and was poured on a casting tray containing mold. The thickness of the PDMS layer was 500 μm. After cooling at room temperature, the PDMS was then peeled from the casting tray and trimmed to size with a blade.

B.2. Bonding Procedure

Prior to bonding of PDMS with a glass substrate, a sharp syringe tip was used to core the inlet and the outlet ports of the micro-channel. PDMS chips were cleaned and plasma surface treatment was performed on the PDMS chips and microscope cover glass slides in a Harrick Plasma PDC-001 plasma cleaner. Cover glass was chosen to reduce reflections of the ultrasound wave. The plasma chamber pressure was allowed to reach 500 mTorr steady state pressure. A single ASM or a group of ASMs were transferred to the well depending on its size. Immediately after the successful transfer, the treated surfaces of the PDMS chips and glass substrates were brought into contact and a Teflon rod was rolled over the PDMS chips to drive out trapped bubbles between mating surfaces and to compress the microcapsule(s) evenly. The bonded chips were placed on a 60 °C hotplate.

A minute after the bonding procedure was complete, it was necessary to provide 0.9% NaCl so that the microcapsules remained viable. The fluidic connection was

provided by a length of Upchurch Scientific 1569 hard polymer tubing that was inserted into each cored hole of the microfluidic chip. After perfusing with NaCl, the connection was severed and the plastic tube was cut to a minimal length to make sure that no gas bubble entered the microfluidic channel under water. The ASMs within the microfluidic device were then exposed to ultrasound.

C. Ultrasound Exposure of ASMs using Optical-Acoustic Setup with the Microfluidic Device

Visualizing the effect of therapeutic ultrasound on the ASMs under the microscope was the primary motivation for setting up a simultaneous optical-acoustic setup. Ultrasound can propagate only through a medium; hence, a tank was setup on the microscope table with DI water in it. The tank was designed to consist of a plastic mold with openings for inserting the transducers at 45° [6]. The focus of the therapeutic transducer was measured using a hydrophone system. The transducer was aligned such that the acoustic and optical foci were in a confocal configuration. ASMs were trapped and compressed in the microfluidic device as described in II.B.3 and the device was placed in the tank on the top of a petri-dish that formed the bottom of the tank. Care was taken to see that the acoustic and optical foci coincided with the channels in the device where the ASMs were placed. Continuous wave (CW) ultrasound was generated for 1-30s with a combination of an arbitrary waveform generator (1281A, Tabor Electronics), 50dB RF amplifier (ENI 240L, ENI), and a high power transducer (Valpey Fisher Inc.) at a center frequency of 2.25 MHz (2" focus, lateral beam-width from hydrophone measurements: 5mm) at acoustic pressures between 130-300 kPa. Ultrasound pressure, center frequency, focal lengths and extents were measured using a custom in-lab acoustic intensity hydrophone measurement system. Light transmission optical microscope images were collected using NIS Elements Nikon Software in the AVI acquisition mode at 50 frames per second (fps) using a region of interest (ROI) within the device where UCAs were seen.

III. RESULTS AND DISCUSSION

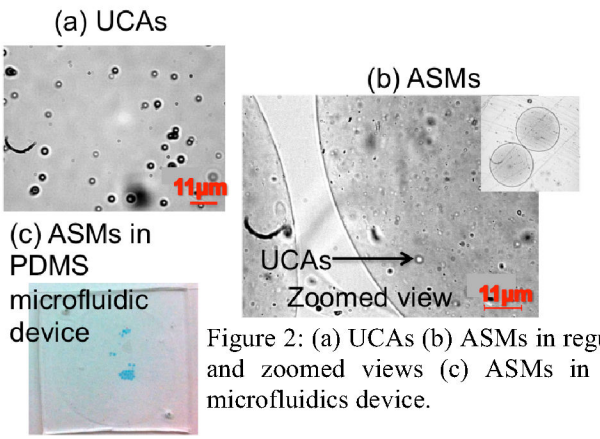

Figure 2: (a) UCAs (b) ASMs in regular and zoomed views (c) ASMs in the microfluidics device.

In Figure 2a, a microscope image of UCAs embedded within gelatin is displayed. They display a central white core with a dark ring. The figure also shows a sample ASM with UCAs and model-drug embedded (Figure 2b). The UCAs within the ASMs can be clearly visualized.

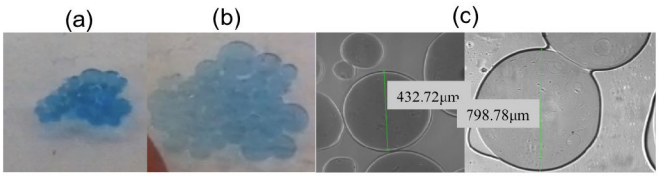

Figure 3: (a-b) Cluster of ASMs squeezed to ~40 microns by the microfluidic device. (c) Microscope image of ASMs before and after microfluidic device compression

The ASMs were trapped successfully in the microfluidic device after successful plasma bonding and are shown in Figures 2c, 3a and 3b. From Figure 3a, b, a cluster of ASMs squeezed to 36.4 μm height through 2 stages is shown - without any structural damage to the capsule membrane. Figure 3c also shown a microscope image of a spherical ASM being compressed. An 84% increase in diameter is seen due to this compression in the plane of the microscope. ASMs were sonicated with continuous wave ultrasound at a central frequency of 2.25 MHz. 2.25 MHz was chosen as the center frequency as the UCA resonant frequency was calculated to be approximately 2.25 MHz. 3 sets of experiments were done. The first set looked at UCA translation near the ASM boundary at 180 kPa acoustic pressure (Figure 4). The second set looked at UCA translation deep within the ASM again at 180 kPa (Figure 5, 6). The third set looked at UCA translation for different acoustic pressures (Figure 7).

For the 1st set, in the first two seconds of sonication, the UCAs enlarged and became darker, indicative of its non-linear volume expansion. Further, as the time of sonication increased, the UCAs began to translate within the microcapsule, possibly due to radiation force. The total distance traveled by the UCA situated farthest from the microcapsule membrane was approximately 5 μm whereas the UCA situated closer to the ASM membrane translated only 2 μm. It can be hypothesized that this was due to the resistance offered by the membrane.

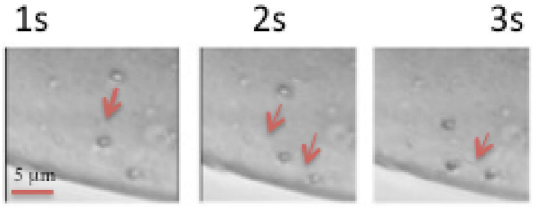

Figure 4: UCA movement towards ASM membrane.

Similar findings were noted by [2, 3], where a single contrast agent could be displaced over 4 microns with a 20 cycle, 180 kPa, 2.25 MHz acoustic pulse. They also established that displacement of the UCA is possibly due to acoustic radiation force (ARF). They have also demonstrated that acoustic radiation force can displace UCAs away from the ultrasound source, resulting in localization of contrast agents along the wall of a vessel both in vitro and in vivo. Here we are using ARF to displace UCAs to the wall of the ASM to aid drug elution.

The translational displacement of UCAs within an ASM for the 2nd set showed a maximum of 333 μm possibly again

due to ultrasound radiation force in the direction of acoustic wave propagation with 30 seconds of sonication. At about 5 seconds, ~90 μm translation was seen. The distance travelled by the UCA deep within the ASM was significantly greater than an ASM at the boundary (boundary: ~5 μm, deep: ~90 μm). Figure 6- top shows the distance travelled with time for a single UCA that was tracked. After the 30th second, the UCA burst and it came to a halt. Since the ultrasound effects were measured within the microfluidic device, vertical movement of the UCAs is limited to 40μm or the height of the device. Most of the movement is seen in the horizontal optical viewing plane. In this experiment, we could not see any secondary radiation force effects.

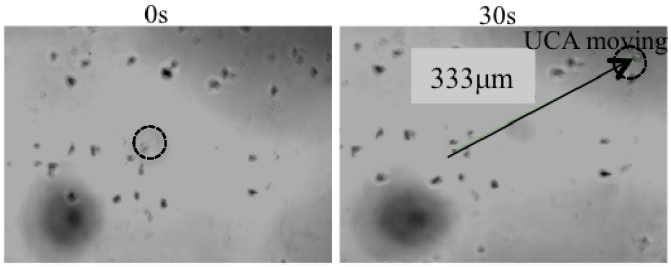

Figure 5: UCA moving within ASM. Arrow tip shows UCA. Other black spots are UCAs that have burst. At 0s we see a shadow of the UCA that becomes clearly visible at 30s. The arrow indicates direction of movement.

As time progressed the distance covered increased. To understand the translational behavior of UCAs due to radiation force for this single experiment, the translation velocity for each 5-second was calculated and plotted (Figure 6 - bottom). The average translation velocity for a UCA was calculated as 13.3 μm/s. Until the 15th second, the translation velocity was decreasing. At 15 seconds, there was a sudden increase in velocity. After this time, velocity decreases and the UCAs burst. We hypothesize that this uneven velocity profile could be due to the Alginate core (cross-linked mesh like structure) that the UCAs encounter within the ASM. For the 3rd set, increase in pressure caused increased movement of the UCA from 6.6 μm to 27 μm for 25s CW exposure. The distance travelled was significantly lower than the 2nd set possibly due to the position of the UCA within the ASM (closer/farther to the membrane).

IV. CONCLUSION

ASMs are being developed to target ischemic areas of large tumors with image guidance. Using our combined optical-acoustic, the ASMs were immobilized within the microfluidic device. ASMs sonicated with continuous wave ultrasound (f_c=2.25 MHz, 3 seconds, 180 kPa) produced an average displacement of 3.5 μm in UCAs near an ASM boundary. This value of displacement increased to ~90 μm when UCAs were tracked deep within the microcapsule. At 30s this displacement was 333 μm after which the UCAs burst. This type of bursting could engage cavitation in the membrane of the ASMs to cause enhanced drug elution. Increase in pressure caused increased translation of the UCAs. In conclusion, UCA translation within ASM due to radiation force was dependent on CW parameters such as exposure time and acoustic pressure. Particularly in this paper UCA movement was restricted to 2D purely for visualization. In clinical scenarios, UCA movement will be 3D but 2D optimized values of acoustic pressure and exposure time could be still applied for the drug delivery process. These two parameters can be carefully optimized in the future to cause these UCAs to travel to the membrane

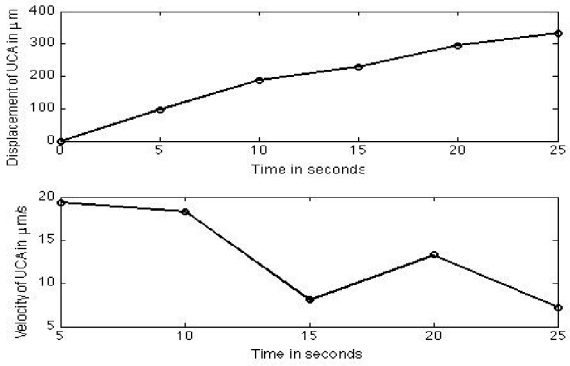

Figure 6: (top) UCA movement over time for CW exposure (180 kPa, 2.25 MHz); (bottom) UCA translational velocity.

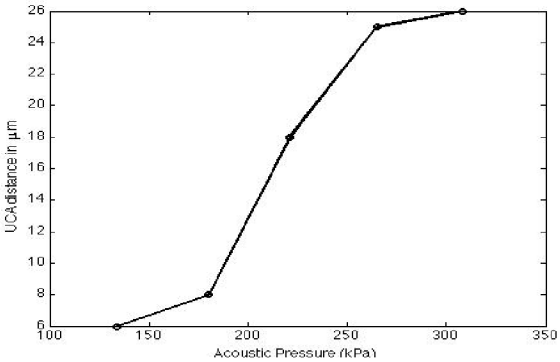

Figure 7: UCA movement with acoustic pressure

boundary to help in the drug elution process. Other parameters like center frequency, pulse repetitive frequency, and duty cycle will also influence the UCA movement and will be a topic of future work.

REFERENCES

[1] Nishiyama, N. 2007. Nanomedicine: Nanocarriers shape up for long life. Nature Nanotechnology 2:203-204.

[2] Bordena, M. A. , H. Zhang, R. J. Gillies, P. A. Dayton, K. W. Ferrara. 2008. A stimulus-responsive contrast agent for ultrasound molecular imaging. Biomaterials 29:597-606.

[3] Shortencarier, M. J., P. A. Dayton, S. H. Bloch, P. A. Schumann, T. O. Matsunaga, K. W. Ferrara. 2004. A method for radiation-force localized drug delivery using gas-filled lipospheres. IEEE transactions on ultrasonics, ferroelectrics, and frequency control 51(7):822-831.

[4] Böhmera, M. R., A. L. Klibanov, K. Tiemann, C. S. Hall, H. Gruell, O. C. Steinbach. 2009. Ultrasound triggered image-guided drug delivery. European Journal of Radiology 70:242-253.

[5] Chang, T. M. S. 2005. Therapeutic Applications of Polymeric Artificial Cells. Nature Reviews - Drug Discovery 4: 221-235.

[6] S. Thirumalai, M. Mobed-Miremadi and M. Keralapura, "Effect of Therapeutic Ultrasound on Acoustically Sensitive Microcapsules", Proceedings of IEEE Engineering Medicine and Biology Society 2011, 4122-4128 (11), 7207-7210.